AD-A101 550   FOREIGN TECHNOLOGY DIV WRIGHT-PATTERSON AFB OH   F/G 5/1

ACTA MECHANICA SINICA (SELECTED ARTICLES),(U)

JUN 81 K CHO, C S TAO, X ZENG

UNCLASSIFIED   FTD-ID(RS)T-0304-81   NL

1 OF 1

AD
A101550

END
DATE
FILMED
8-81
DTIC

JS

AD A101550

FTD-ID(RS)T-0304-81

2

FOREIGN TECHNOLOGY DIVISION

AIR FORCE SYSTEMS COMMAND

ACTA MECHANICA SINICA
(Selected Articles)

FOREIGN TECHNOLOGY DIVISION

Approved for public release;
distribution unlimited.

81 7 17 063

EDITED TRANSLATION

(14) FTD-ID(RS)T-0304-81 (11) 26 Jun[redacted]81

MICROFICHE NR: FTD-C-81-000578

(6) ACTA MECHANICA SINICA (Selected Articles),

(10) Kao /Cho
Chao Shu /Tao
[redacted]Xin-Chuan

English pages: 20

(21) Edited Tran...

~~Source:~~ Acta Mechanica Sinica, Nr. 2, 1980,
pp. 129-137, [redacted]

(12)

Country of origin: (China) n2 p129-137

Translated by: SCITRAN
F33657-78-D-0619

Requester: FTD/TQTA

Distribution limited to U. S. Government Agencies Only; Proprietary (Copyright) Information; Other requests for this document must be referred to FTD/STINFO.

THIS TRANSLATION IS A RENDITION OF THE ORIGINAL FOREIGN TEXT WITHOUT ANY ANALYTICAL OR EDITORIAL COMMENT. STATEMENTS OR THEORIES ADVOCATED OR IMPLIED ARE THOSE OF THE SOURCE AND DO NOT NECESSARILY REFLECT THE POSITION OR OPINION OF THE FOREIGN TECHNOLOGY DIVISION.	PREPARED BY: TRANSLATION DIVISION FOREIGN TECHNOLOGY DIVISION WP-AFB, OHIO.

TABLE OF CONTENTS

THE THEORY OF GAIN, INTENSITY AND POWER OF GAS LASERS

Kao Cho* and Chao Shu Tao

ABSTRACT

The particle thermal velocity distribution is introduced into the speed equation to obtain the relations between gain, intensity and power of gas lasers. This paper reached the same conclusions as reference [1] under uniform broadening conditions. The results were simplified to become the well known non-flowing gas laser equations when the flow speed is zero.

In the analysis, the change in the reflectivity of the mirror and the degree of excitation as a function of time of gases in the upstream region of the optical chamber were considered with respect to both continuous and pulsed gas-flowing CO_2 lasers.

I. INTRODUCTION

In the analysis of a gas-flowing CO_2 laser, under the conditions that gain is equal to consumption, the solution to the speed equations put on line [1,2] applies only to the uniform broadening situation. Under conditions that both uniform and non-uniform broadenings exist, reference [3] made an analysis. In addition, the semi-empirical analyses of gas flow lasers [4,5] suggested that it was possible to apply some theory in the treatment of non-flow gas lasers in the explanation of experimental results with gas flow lasers. However, theoretical results were already available [1-3] for gas flow lasers. But they cannot be reduced to

* This paper was received on April 7, 1978.

non-flow gas laser equations when the flow speed approaches zero.

The introduction of thermal velocity distribution to the speed equation will enable us to obtain the theoretical relations between the gain, intensity and power of gas flow lasers. When the flow speed equals zero, these relations reduce to the familiar non-flow gas laser equations. Under uniform broadening, the results are the same as those reported in references [1,2]. It must be pointed out that, vigorously speaking, particle thermal velocity distribution cannot be brought into the speed equations. However, this technique very simply provided desirable results and will serve as a basis for further analysis.

II. ASSUMPTIONS AND BASIC EQUATIONS

Let us assume the following: The optical axis is perpendicular to the direction of gas-flow, gas passage is rectangular in cross-section and plane parallel mirrors are placed on either side of the passage as shown in Figure 1. The variations of gas parameters u, p and T inside the optical chamber can be neglected. The effect of the boundary layer is also negligible [7].

The pump region and the optical chamber are separated in order to analyze the "flow broadening" pulse width of the pulsed pump upstream of the optical chamber.

The working energy levels of the CO_2-N_2 laser system can be described as the five-energy level model shown in Figure 2. Energy level 1 includes the symmetric and bending levels of CO_2. The number of particles transported from energy level i to j, due to inelastic collisions, in a unit time is $K_{ij}N_i$; N_i is the density of particles at energy level i. Speed K_{ij} (unit sec^{-1}) satisfies the following:

$$K_{32}, K_{23}, K_{10} \gg K_{21} > K_{0j} (j = 1, 2, 3) \qquad (2.1)$$

With constant u, p and T, the non-constant speed equations and the radiation exchange equation are:

$$\left.\begin{aligned}
&\frac{\partial N_3}{\partial t} + u\frac{\partial N_3}{\partial x} = w_3 - K_{32}N_3 + K_{23}N_2 \\
&\frac{\partial N_2}{\partial t} + u\frac{\partial N_2}{\partial x} = w_2 + K_{32}N_3 - (K_{23} + K_{21})N_2 - \frac{J}{\mathrm{ch}\nu}(B'_{21}f_2N_2 - B'_{12}f_1N_1) \\
&\frac{\partial N_1}{\partial t} + u\frac{\partial N_1}{\partial x} = w_1 + K_{21}N_2 - K_{10}N + \frac{J}{\mathrm{ch}\nu}(B'_{21}f_2N_2 - B'_{12}f_1N_1) \\
&\qquad N_2 + N_1 + N_0 = \text{常数} \\
&\qquad\quad N_{0'} + N_3 = \text{常数}
\end{aligned}\right\} \quad (2.2)$$

$$\frac{\partial J}{\partial t} + cl\,\mathrm{grad}\,J = (B'_{21}f_2N_2 - B'_{12}f_1N_1)J \qquad (2.3)$$

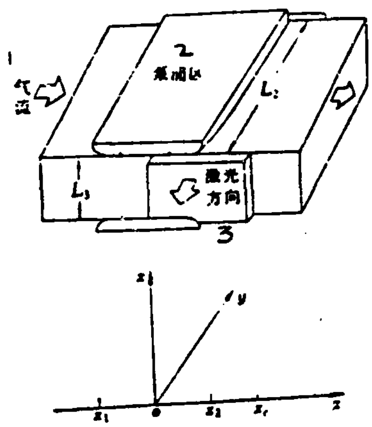

Figure 1. Schematic diagram of a transverse gas flow laser and coordinate system.
(pump zone $x_1 \leq x \leq x_2$; optical chamber $0 \leq x \leq x_c = L$)
1—gas flow; 2—pump zone;
3—laser direction

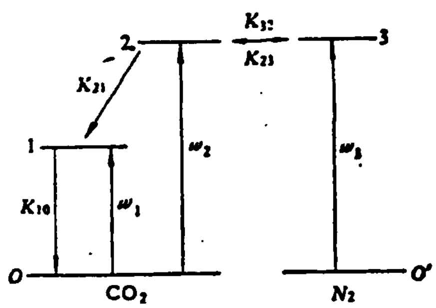

Figure 2. Energy levels of the CO_2-N_2 laser system and relaxation processes.

where t is time, u is flow-speed, w_i (i=1,2,3) is pump speed; c is speed of light, h is the Boltzmann constant, ν is light frequency, J is radiation intensity; f_i (i=1,2) is the fraction of particles in N_i with laser action, B'_{21} is the speed of excited particles with Doppler frequency ν' under the influence of radiation with frequency ν.

$$B'_{21} = B_{21}\frac{2/\pi\Delta\nu_N}{1+\left[\frac{2(\nu'-\nu)}{\Delta\nu_N}\right]^2}, \quad B'_{12} = \frac{g_2}{g_1}B'_{21} \tag{2.4}$$

g_i (i=1,2) is the statistical weight of energy level; $\Delta\nu_N$ is the full width at half peak of the uniform broadening curve. I is the direction of light propagation. The intensity satisfies the following boundary conditions

$$\left.\begin{array}{l} y = 0 \;\; J_0^+ = R_1 J_0^-, \;\; R_1 = 1 - a_1 - t_1 \\ y = L_2 \;\; J_{L_2}^- = R_2 J_{L_2}^+, \;\; R_2 = 1 - a_2 - t_2 \end{array}\right\} \tag{2.5}$$

R_i, a_i and t_i (i=1,2) are the reflection, absorption and transmission coefficients of the mirrors on both sides respectively. J^+ and J^- are the photon energy flows in the positive and negative y direction and we have $J = J^+ + J^-$.

III. SOLUTION

On the left hand of (2.3), with the exception of $\frac{\partial J}{\partial y}$ other terms are small enough to be negligible. Therefore, from (2.3) and (2.5), we get

$$g = \frac{1}{L_2}\int_0^{L_2}\frac{1}{c}(B'_{21}f_2N_2 - B'_{12}f_1N_1)dy = \frac{-1}{2L_2}\ln R_1R_2 \tag{3.1}$$

Because [1] $J_{max}/J_{min} = 2\sqrt{R}/(1+R)$, $R = \min(R_1, R_2)$, , therefore, the variation of J along the y direction can be neglected when $R \lesssim 0.6$. From (2.3) and (2.5), we obtain

$$gI = \frac{1}{L_2}\int_0^{L_2}\frac{1}{c}(B'_{21}f_2N_2 - B'_{12}f_1N_1)Jdy = \frac{1}{L_2}(J^+_{L_2} - J^-_{L_2} + J^-_0 - J^+_0) \tag{3.2}$$

$$J_0 = J_0^-(1+R_1) = \frac{gIL_2(1+R_1)\sqrt{R_2}}{(\sqrt{R_1}+\sqrt{R_2})(1-\sqrt{R_1R_2})}, \quad I = \frac{1}{L_2}\int_0^{L_2}Jdy \tag{3.3}$$

The g here is the average gain coefficient with respect to y. Equation (3.1) is the condition required for gas flow laser resonance. Generally, R_i and g vary with x.

The solution to the speed equations is obtained as follows: First take the integral average of (2.1) with respect to y and then carry out these mathematical transformations:

$$\xi = \frac{x}{u}, \quad \zeta = t - \frac{x}{u} \tag{3.4}$$

(2.1) is then changed into:

$$\left.\begin{aligned}
&\frac{\partial^2 n_b}{\partial \xi^2} + (K_{32} + S_1 K_{2r} + S_2 K_{10}) \frac{\partial n_b}{\partial \xi} + S_2 K_{32} K_{10} n_b \\
&\qquad = K_{32} \sum_{i=1}^{3} w_i + \frac{\partial (w_1 + w_2)}{\partial \xi} + S_0 \left[(K_{10} - K_{23}) \frac{\partial g}{\partial \xi} + K_{32} K_{10} g \right] \\
&\frac{\partial^2 n_3}{\partial \xi^2} + (K_{32} + S_1 K_{23} + S_2 K_{10}) \frac{\partial n_3}{\partial \xi} + S_2 K_{32} K_{10} n_3 \\
&\qquad = S_1 K_{23} \sum_{i=1}^{3} w_i + S_2 K_{10} w_3 + \frac{\partial w_3}{\partial \xi} + S_0 K_{23} \left(\frac{\partial g}{\partial \xi} + K_{10} g \right)
\end{aligned}\right\} \tag{3.5}$$

where

$$n_b = n_1 + n_2, \quad n_2 = S_1 n_b + S_0 g, \quad n_1 = S_2 n_b - S_0 g \tag{3.6}$$

$$S_0 = \frac{c}{B'_{21} f_2 + B'_{12} f_1}, \quad S_2 = \frac{B'_{21} f_2}{B'_{21} f_2 + B'_{12} f_1}, \quad S_1 + S_2 = 1 \tag{3.7}$$

$$n_i = \frac{1}{L_2} \int_0^{L_2} N_i \, dy$$

Let $g = g(\zeta) e^{\delta \xi}$, and then obtain the solution to (3.5) as:

$$\left.\begin{aligned}
n_b &= n_{bp} + S_0 g n_{bg} + \sum_{\substack{i=1 \\ (j \neq i,\ j=1,2)}}^{2} \frac{e^{-\lambda_i \xi}}{\lambda_j - \lambda_i} \{ (w_1 + w_2 - \lambda_i n_{bp}) + K_{12} n_3^0(\zeta) \\
&\quad + (\lambda_i - S_1 K_{2r} - S_2 K_{10}) n_b^0(\zeta) + S_0 g [(K_{10} - K_{23}) - (\lambda_i + \delta) n_{bg}] e^{-\delta \xi} \} \\
n_3 &= n_{3r} + S_0 g n_{3g} + \sum_{\substack{i=1 \\ (j \neq i,\ j=1,2)}}^{2} \frac{e^{-\lambda_i \xi}}{\lambda_j - \lambda_i} \{ (w_3 - \lambda_i n_{3p}) + (\lambda_i - K_{32}) n_3^0(\zeta) \\
&\quad + S_1 K_{23} n_b^0(\zeta) + S_0 g [K_{23} - (\lambda_i + \delta) n_{3g}] e^{-\delta \xi} \}
\end{aligned}\right\} \tag{3.8}$$

The superscript 0 on the right represents the distribution of the corresponding quantity at $\xi = 0$ (i.e., x=0). δ is a constant and w_i is another constant.

$$\lambda_{1,2} = \frac{1}{2} [(K_{32} + S_1 K_{23} + S_2 K_{10}) \pm \sqrt{(K_{32} + S_1 K_{23} + S_2 K_{10})^2 - 4 S_2 K_{32} K_{10}}]$$

$$n_{b_g} = \frac{(K_{10} - K_{21})\delta + K_{32}K_{10}}{\delta^2 + (K_{32} + S_1K_{23} + S_2K_{10})\delta + S_2K_{32}K_{10}},$$

$$n_{3_g} = \frac{K_{21}(K_{10} + \delta)}{\delta^2 + (K_{32} + S_1K_{23} + S_2K_{10})\delta + S_2K_{32}K_{10}}$$

$$n_{b_p} = \begin{cases} \frac{1}{S_2K_{10}} \sum_{i=1}^{3} w_i & 0 \leqslant \xi \leqslant \xi_2 = \frac{x_2}{u} > 0 \\ 0 & \xi > \xi_2 \end{cases}$$

$$n_{3_p} = \begin{cases} \frac{S_2K_{10}w_3 + S_1K_{23} \sum_{i=1}^{3} w_i}{S_2K_{32}K_{10}} & 0 \leqslant \xi \leqslant \xi_2 \\ 0 & \xi > \xi_2 \end{cases}$$

(3.8) is the solution when $\lambda_1 \neq \lambda_2$. Similarly, a solution when $\lambda_1 = \lambda_2$ can be obtained. It will not be discussed here. The initial distribution at x = 0 is explained as follows: (1) initial distribution can be obtained from the solution to (2.2) under radiationless condition $J \equiv 0$. The radiationless solution is not going to be written here. Under continuous pumping at the upstream of the optical chamber, $n_i^0(\zeta)|_{\xi=0} = n_i^0(t)|_{x=0} =$ constant. When pulsed pumping is used, $n_i^0(t)|_{x=0}$ varies with t. (2) the radiationless solution usually generally does not satisfy (3.1). However, since $\frac{2L_2}{c(1 - R_1R_2)} \ll K_{32}^{-1}, K_{10}^{-1}, \frac{n_0}{w_i},$, the inelastic exchange of collision within the time period $\frac{2L_2}{c(1-R_1R_2)}$ cannot be completed. In addition, since $\frac{2L_2u}{c(1 - R_1R_2)} \ll L_1,$ at $\xi = 0$ we get:

$$n_b^0 = n_2^0(\zeta) + n_1^0(\zeta), \quad n_3^0 = n_3^0(\zeta) \tag{3.9}$$

where $n_i^0(\zeta) = n_i^0(t)|_{x=0}\ (i = 1, 2, 3)$ which can be obtained from the radiationless solution. (3) generally, since $K_{32}, K_{10} \gg K_{21}, \frac{u}{L_1},$ therefore $K_{32}n_3^0(\zeta) = K_{21}n_2^0(\zeta)$.

From (2.2) and (3.6), gI can be obtained

$$\frac{gI}{h\nu} = S_2w_2 - S_1w_1 + S_2K_{32}n_3 - S_1fn_b - S_0g(\delta + K_{21} + S_2K_{23} + S_1K_{10})$$
$$- \frac{2}{\pi\Delta\nu_N} \frac{K_0I_i}{h\nu} \exp\left\{-\left[\frac{2(\nu' - \nu_0)\sqrt{\ln 2}}{\Delta\nu_D}\right]^2\right\}$$
$$- \left(1 + \left[\frac{2(\nu' - \nu)}{\Delta\nu_N}\right]^2\right) \frac{gI_i}{h\nu} \tag{3.10}$$

where
$$f = K_{21} + S_2 K_{23} - S_2 K_{10} \tag{3.10}$$

$$\frac{2}{\pi \Delta\nu_N} \frac{K_0 I_s}{h\nu} = \left(\omega_{20} + \omega_{10} - \frac{S_1 K_{21}}{S_2 K_{10}} \sum_{i=1}^{3} \omega_{i0}\right) + \sum_{\substack{i=1 (j\neq i \\ j=1,2)}}^{2} \frac{e^{-\lambda_i \xi}}{\lambda_j - \lambda_i} \{S_2 K_{32}(\omega_{30} - \lambda_i n_{3p})$$
$$- S_1 f(\omega_{10} + \omega_{20} - \lambda_i n_{bp}) + [S_2 K_{32}(\lambda_i - K_{32}) - S_1 f K_{32}] n_{30}^0(\zeta)$$
$$+ [S_1 S_2 K_{23} K_{32} - S_1 f(\lambda_i - S_1 K_{23} - S_2 K_{10})] n_{b0}^0(\zeta)\}$$
$$\frac{I_s}{h\nu} = \frac{\pi \Delta\nu_N}{2} \frac{c S_2}{B_{21} f_2} \Big\{(K_{21} + S_2 K_{23} + S_1 K_{10} + \delta - S_2 K_{32} n_{3g} + S_1 f n_{bg})$$
$$- \sum_{\substack{i=1 (j\neq i, \\ j=1,2)}}^{2} \frac{e^{-(\lambda_i+\delta)\xi}}{\lambda_j - \lambda_i} (S_2 K_{32}[K_{23} - (\lambda_i + \delta) n_{3g}] - S_1 f[(K_{10} - K_{23})$$
$$- (\lambda_i + \delta) n_{bg}])\Big\}$$

In the derivation of (3.10), it has been assumed that a quasi-equilibrium was reached and partial Maxwell velocity distribution was established, i.e.,

$$\omega_i = \omega_{i0} \exp\left\{-\left[\frac{2(\nu' - \nu_0)\sqrt{\ln 2}}{\Delta\nu_D}\right]^2\right\},$$
$$n_i = n_{i0} \exp\left\{-\left[\frac{2(\nu' - \nu_0)\sqrt{\ln 2}}{\Delta\nu_D}\right]^2\right\}$$

where ν_0 is the center frequency of the Doppler line and $\Delta\nu_D$ is the full width at half peak in the Doppler line.

IV. GAIN, INTENSITY AND POWER

Using (3.10) under conditions that the light frequency equals the Doppler center frequency (i.e., $\nu = \nu_0$), we get

$$g = \frac{K_0}{\pi} \int_{-\infty}^{\infty} \frac{\exp(-z^2\eta^2)}{1 + z^2 + I/I_s} dz = \frac{K_0 \exp\left[\eta^2\left(1 + \frac{I}{I_s}\right)\right]}{\sqrt{1 + I/I_s}} \left\{1 - \mathrm{erf}\left(\eta\sqrt{1 + \frac{I}{I_s}}\right)\right\} \tag{4.1}$$

where $\eta = \frac{\Delta\nu_N}{\Delta\nu_D}\sqrt{\ln 2}$, $z = \frac{2(\nu' - \nu_0)}{\Delta\nu_N}$, erf is the probability integral. When non-uniform broadening dominates, i.e., $\eta \to 0$, (4.1) becomes

$$g = \frac{K_0(\xi, \zeta)}{\sqrt{1 + I/I_s(\xi)}} \tag{4.2}$$

When uniform broadening dominates, i.e., $\eta\to\infty$ (4.1) becomes

$$g=\frac{g_0(\xi,\zeta)}{1+I/I_s(\xi)},\quad g_0=\frac{K_0}{\eta\sqrt{\pi}} \tag{4.3}$$

It is defined as the partial saturation intensity K_0 and g_0 are non-uniform and uniform broadening saturation gain coefficients, respectively. When the gain is equal to the loss, the above equation also applies. It becomes the familiar theory [6] on non-flow gas lasers. When $\lambda_s\xi \gg 1$

$$I_s\to\bar{I}_s=\frac{\pi\Delta\nu_N}{2}\frac{ch\nu S_2}{B_{21}f_2}\frac{K_{21}K_{32}K_{10}+\delta[K_{21}K_{32}+(K_{12}+K_{21}+K_{31})K_{10}]}{S_2K_{32}K_{10}+(K_{32}+S_1K_{21}+S_2K_{10})\delta} \tag{4.4}$$

$$K_0I_s\to\bar{K}_0\bar{I}_s=\frac{\pi\Delta\nu_N h\nu}{2}\left(w_{20}+w_{30}-\frac{S_1K_{21}}{S_2K_{10}}\sum_{i=0}^{3}w_{i0}\right)$$

Equation (4.4) omits δ^2 as a higher order term. From (4.1)-(4.3), it is easy to obtain the radiation intensity in the optical chamber. The transmitted intensity J_t is

$$J_t=J_0^-t_1+J_{L_2}^+t_2=\frac{gIL_2(t_1\sqrt{R_2}+t_2\sqrt{R_1})}{(\sqrt{R_1}+\sqrt{R_2})(1-\sqrt{R_1R_2})} \tag{4.5}$$

Integrating J_t with reppect to x and t, we get the power. For single end output with the other end as a no-loss total reflection mirror (i.e., $R_2 = 1$), we get

$$P=\frac{V}{L_1(\zeta-\zeta_0)}\int_{\zeta_0}^{\zeta}\int_0^{\xi_e}\frac{t_1u}{a_1+t_1}\frac{K_0I\exp\left[\eta^2\left(1+\frac{I}{I_s}\right)\right]}{\sqrt{1+I/I_s}}\left[1-\mathrm{erf}\left(\eta\sqrt{1+\frac{I}{I_s}}\right)\right]d\xi d\zeta\Big|_{\xi=0} \tag{4.6}$$

where $V = L_1L_2L_3$ is the volume of the optical chamber. For $\eta\gg 1$, (4.6) becomes

$$P=\frac{uVt_1}{L_1(\zeta-\zeta_0)(a_1+t_1)}\left\{\int_{\zeta_0}^{\zeta}\int_0^{\xi_e}g_0I_sd\xi d\zeta\Big|_{\xi=0}+\frac{\ln R_1^0}{L_2}\int_{\zeta_0}^{\zeta}\int_0^{\xi_e}I_se^{\delta\xi}d\xi d\zeta\Big|_{\xi=0}\right\}$$
$$=\frac{t_1VI_s^*}{L_2(a_1+t_1)}(g_0^*L_2+\ln R_1^0) \tag{4.7}$$

where

$$I_s^*=\frac{u}{L_1(\zeta-\zeta_0)}\int_{\zeta_0}^{\zeta}\int_0^{\xi_e}I_se^{\delta\xi}d\xi d\zeta\Big|_{\xi=0},$$

$$g_0^*L_2=\frac{L_2\int_{\zeta_0}^{\zeta}\int_0^{\xi_e}g_0I_sd\xi d\zeta\Big|_{\xi=0}}{\int_{\zeta_0}^{\zeta}\int_0^{\xi_e}I_se^{\delta\xi}d\xi d\zeta\Big|_{\xi=0}} \tag{4.8}$$

I_s^* and g_o^* can be considered as the gain coefficients of uniform saturation intensity and non-uniform saturation intensity, respectively. They are average values with respect to time and space. (4.7) is in the same form as the Rigrod equation for non-flow gas lasers. Substituting (3.10) into (4.8), I_s^* and g_o^* can be obtained:

$$I_s^* = \frac{\pi \Delta \nu_N}{2} \frac{ch\nu u S_2}{B_{21} f_2 L_1} \Big\{ (K_{21} + S_2 K_{23} + S_1 K_{10} + \delta - S_2 K_{32} n_{3g} + S_1 f n_{bg}) \frac{e^{\delta L_1/u} - 1}{\delta}$$
$$- \sum_{\substack{i=1 (j \neq i \\ j = 1,2)}}^{2} \frac{1 - e^{-\lambda_i L_1/u}}{\lambda_i (\lambda_j - \lambda_i)} (S_2 K_{32} [K_{32} - (\lambda_j + \delta) n_{3g}]$$
$$- S_1 f [(K_{10} - K_{23}) - (\lambda_j + \delta) n_{bg}]) \Big\} \tag{4.9}$$

The expression for g_o^* is going to be omitted. The t_1^* corresponding to the maximum power out is obtained based on $\frac{\partial P}{\partial t_1} = 0$ For $\delta = 0$, we get

$$\frac{t_1^*}{a_1} = \frac{1 - a_1 - t_1^*}{a_1 + t_1^*} [g_0^* L_2 + \ln(1 - a_1 - t_1^*)] \tag{4.10}$$

From (4.7) and (4.10), the maximum power output P* is

$$P^* = \frac{V I_s^* (t_1^*)^2}{L_2 a_1 (1 - a_1 - t_1)} = \frac{(t_1^*)^2}{a_1 (1 - a_1 - t_1)} \frac{uV}{L_1 L_2 (\zeta - \zeta_0)} \int_{\zeta_0}^{\zeta} \int_0^{t_c} I_s d\xi d\zeta \Big|_{t=0} \tag{4.11}$$

The above equation has the same form as the Rigrod equation [6]. For $\eta \ll 1$ (non-uniform broadening), the same discussion can be made.

V. ANALYSIS OF PARAMETERS

I_s is proportional to the square of the pressure P^2. It is not related to the pumping rate and the degree of excitation of the gas at the inlet of the optical chamber. From (3.10) we know that I_s decreases monotonically with $\frac{x}{u}$ from its maximum I_s

max at x = 0 to $\bar{I}_s$ (see equation (4.4)).

$$I_{s,\max} = I_s|_{x=0} = (K_{21} + S_2K_{23} + S_1K_{10} + \delta)\frac{c h\nu S_2}{B_{21}f_2}\frac{\pi\Delta\nu_N}{2} \tag{5.1}$$

Increasing the flow speed (leaving other parameters unchanged), we found that $I_{s,max}$ remained the same but I_s and $\bar{I}_s$ increased significantly (see example). The variation in reflectivity $R_1 = (R_1^o)^{\delta\xi}$ significantly affects I_s. The reasonable limits for δ was derived to be:

$$|\delta| < \min(\lambda_1, \lambda_2) \text{ for } |\delta| = O(K_{21}) \tag{5.2}$$

From (4.4) we know that $\delta \approx -\dfrac{K_{21}K_{32}}{K_{32} + K_{23}}, \bar{I}_s \approx 0$. This is because when $\delta < 0$ R_1 increases monotonically with $\frac{x}{u}$ and t_1 monotonically decreases. When t_1 is reduced to zero, light radiation is forced to stop; when $\delta > 0$ $\bar{I}_s|_{\delta>0} >$ or$\gg$ $)\bar{I}_s|_{\delta=0}$.
In gas-flow lasers, K_o and g_o are parameters of I_s which are related to the mirror surface conditions. Only when u = 0 and $\delta = 0$, these parameters will have the physical meaning of corresponding parameters for non-flow steady-state gas lasers. It demonstrates the characteristics of the non-steady state nature of gas-flow lasers. The parametric dependence of I_s^* is identical to that of I_s.

If the pumping rate w_i is proportional to p, then the non-saturation gain coefficient K_o is not related to p and g_o is inversely proportional to p. K_o, g_o and w_i are proportional to the degree of excitation of the gas at the inlet of the optical chamber. From (3.10) and (4.4), we know that for pumping upstream of the optical chamber, for $\delta \geq 0$, g_o decreases monotonically and for $\delta < 0$, g_o increases monotonically. For pumping inside the optical chamber, we get from (4.4)

$$\bar{K}_0 = \left(w_{20} + w_{30} - \frac{S_1K_{21}}{S_2K_{10}}\sum_{i=1}^{3} w_{i0}\right) \cdot \frac{B_{21}f_2[S_2K_{32}K_{10} + (K_{32} + S_1K_{23} + S_2K_{10})\delta]}{cS_2\{K_{21}K_{32}K_{10} + [K_{21}K_{32} + (K_{32} + K_{23} + K_{21})K_{10}]\delta\}} \tag{5.3}$$

Therefore, for the same pumping conditions , $\bar{K}_0|_{\delta>0} < (\text{or} \ll) \bar{K}_0|_{\delta=0}$.

Power P is proportional to p, u, pumping speed and the degree of excitation at the inlet of the optical chamber. When reflectivity is constant and $\delta = 0$, the maximum power output P* is proportional to p^2 and mirror area.

VI. EXAMPLE

For a $CO_2/N_2/H_e$ gas mixture, the speed constants are tabulated as follows [8]:

speed constants at T = 300°K

N_{He}/N	K_{10}/p (TORR^{-1}sec^{-1})	K_{21}/p (TORR^{-1}sec^{-1})	K_{23}/p (TORR^{-1}sec^{-1})	K_{32}/K_{23}
0	8.8×10^2	1.23×10^2	1.67×10^4	
0.3	1.2×10^3	1.03×10^2	1.16×10^4	N_{CO_2}/N_{N_2}
0.5	1.9×10^3	9.6×10^1	8.3×10^4	

From information in reference [8], we get

$$\frac{S_2}{S_0} = \frac{\lambda_0^2\theta_r}{4\pi\tau_{21}\nu_c}\,\frac{2(2l+1)}{T}$$

$$\cdot \exp\left[-l(l+1)\frac{\theta_r}{T}\right] \approx \frac{718}{NT}\,(\text{cm}^2)$$

S_1/S_2 is also a function of temperature and degree of excitation. When T = 300°K and degree of excitation is not too high, $\frac{S_1}{S_2} \approx 0.04$.

The variation of I_s with $\frac{\lambda_2 c}{\mu}$ $(\lambda_2 < \lambda_1)$ is shown in Figure 3. I_s approximately is in the $10^3 - 10^1$ watt/cm^2 region which is consistent with experimental results [9]. The calculated curve of I_s proved the analytical conclusion given in the previous section. When $\delta = \frac{\lambda_2}{5}$, I_s is 10 times larger than $I_s|_{\delta=0}$.

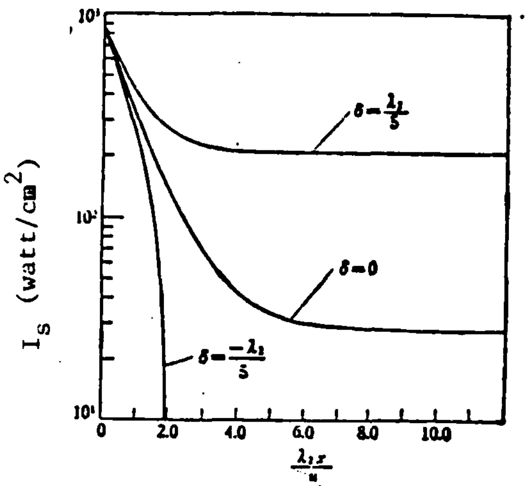

Figure 3. Variation of I_s with $\frac{\lambda_2 x}{u}$

$T = 300K$, $p = 30$ torr $CO_2/N_2/He = 1/4/5$

Figures 4 and 5 show the change of g_0 and I with $\frac{\lambda_2 x}{u}$ and $\frac{ut}{L_1}$, respectively. The pulsing time of the pump vs. time can be expressed as the variation of n_2^0 with $\frac{ut}{L_1}$. g_0 and I are like "waves" propagating in the right direction. Straight lines $\frac{tu}{L_1} - b\frac{\lambda_2 x}{u} = 0$ and $= 1$ are the front and back surfaces of the wave where $b = \frac{u}{\lambda_2 L_1}$. From Figures 4 and 5, we know that along a straight line $\frac{tu}{L_1} - b\frac{\lambda_2 x}{u} = H = \text{const}$ $0 < H < 1$, the variation of g_0 is slower than that of I.

For continuous pumping, when R_1 = const, $\bar{g}_0$* monotonically gradually decreases with $\frac{\lambda_2 x}{u}$. When $\frac{\lambda_2 x}{u} = 10$, g_0^* is approximately 0.8. When $\delta = \frac{\lambda_1}{5}$ $\bar{g}_0$* more significantly monotonically declines. When $\frac{\lambda_2 x}{u} = 10$ g_0^* is about 0.1. When $\delta = \frac{-\lambda_1}{5}$, $\bar{g}_0$* increases with $\frac{\lambda_2 x}{u}$ and I_s* decreases with $\frac{\lambda_2 x}{u}$. Note that $\bar{g}_0$* and I_s* do not have any obvious physical meanings. From Figures 4 and 6, it can be seen that when R is constant, the variations of g_0 and g_0* with $\frac{x}{u}$ are slow regardless of whether continuous or pulsed pumping is used. This serves as a theoretical basis for the calculation of gas flow laser power using an average value of the gain coefficient and the non-flow gas laser equation as suggested in references [5,7].

Gas laser power calculated here agrees with that reported in reference [1] (see Figure 7). $\frac{\lambda_2 x}{u}$ represents the fraction of effective vibrational energy taken. For the calculation parameters in Figure 7, when $\frac{\lambda_2 x}{u} \approx 5$, the effective energy is completely used.

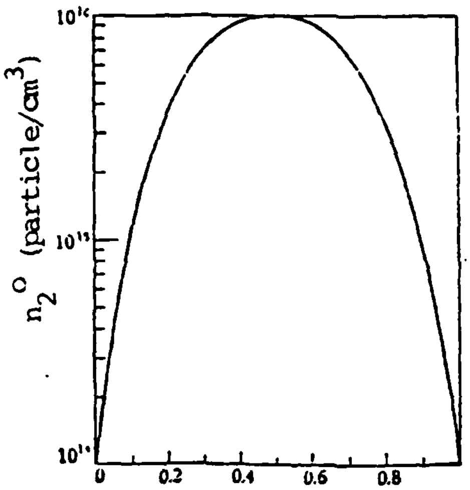

Figure 4.1. The variation of n_2^o with $\frac{ut}{L}$ at inlet of optical chamber.
$T = 300K$, $p = 30$ torr, $\delta = 0$, $g_{s-o} = 2\times10^{-3}$ cm^{-1}, $CO_2/N_2/He = 1/4/5$

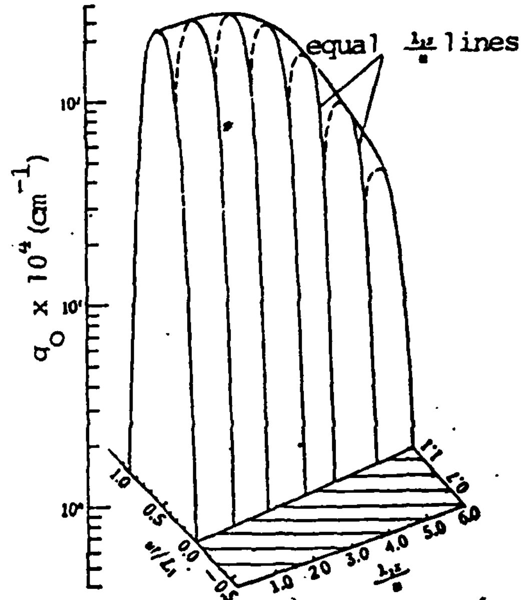

Figure 4. g_o vs. $\frac{\lambda_2 x}{u}$ and $\frac{ut}{L_1}$ curves.

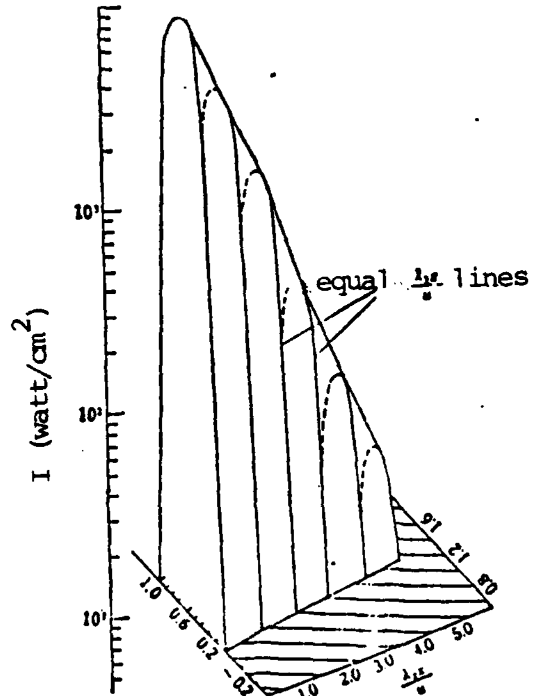

Figure 5. I vs. $\frac{\lambda_2 x}{u}$ and $\frac{ut}{L_1}$ curve.

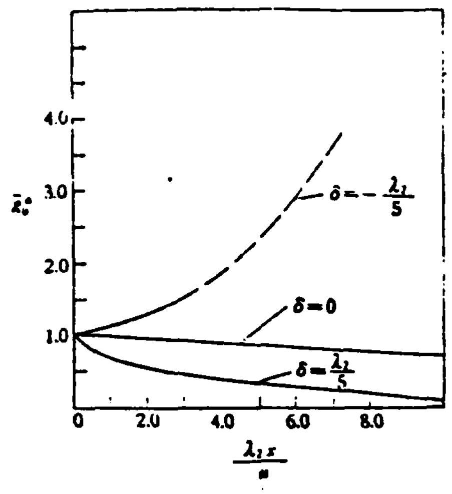

Figure 6. Unified average non-staturation gain $\bar{g}_o$* vs. $\frac{\lambda_2 x}{u}$

T=300°K p=30 torr
$CO_2/N_2/He=1/4/5$

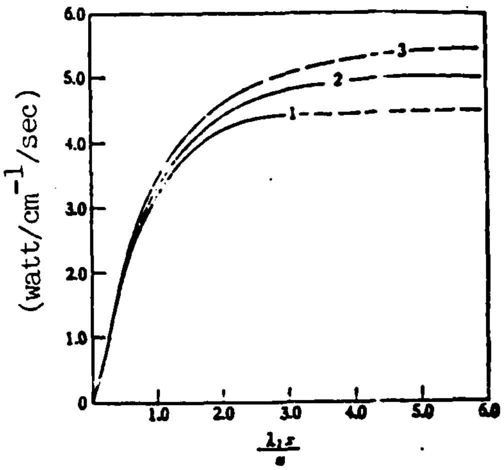

Figure 7. Gas laser output power $\frac{p}{uA}$ vs. $\frac{\lambda_2 x}{u}$

1. $\delta = \frac{\lambda_2}{5}$, 2. $\delta=0$, 3. $\delta = -\frac{\lambda_2}{5}$,
T=300°K, p=30 torr
$CO_2/N_2/He=1/4/5$ $\frac{\varepsilon_1}{a_1+\varepsilon_1} = 0.7$,
$g_{x=0} = 2\times10^{-3}\,cm^{-1}$ $n_2^o = 10^{16}$ particle/cm^3

REFERENCES

[1] Cool, T. A., *J. Appl. Phys.*, 40, 9(1969), 3563.

[2] Пименов, В. П., и др., *Кван. элек.*, 4, 2 (1977), 355.

[3] Goela, J. S., et al., *AIAA J.*, 13, 12(1975), 1629.

[4] Davis, J. W., et al., *AIAA Paper*, No. 72—722.

[5] Lee, G., et al., *AIAA J.*, 10, 1(1972), 65.

[6] Maitland, A., et al., *Laser Physics*, 1969.

[7] Kao Chi, Physics Journal, 27, 4 (1978), p. 340.

[8] Hoffman, A. I., et al., *IEEE J.*, QE-8 (1972), 46.

[9] Cheo, P. K., Lasers, 3, Chap. 2, New York, Dekker 1966.

CONTACT PROBLEMS OF LONG RIGID FRAME FOOTING ON ELASTIC FOUNDATION

Zeng Xin-Chuan*

(The Seismological Brigade of Wuhan, National Seismological Bureau)

In reference [1], Galin solved the contact problems between two flat bottom pressure heads under center load and elastic semi-flat foundation with friction present. The distribution of stress along the contact surface was obtained. In this paper, the author used the Muskhelishvili method [2] to attack the contact problems of long rigid frame footing under off-center load on an elastic foundation. For simplicity in the calculation, it was assumed that the contact between the footing and the foundation is frictionless.

The action of an off-center load (Figure 1) is equivalent to the combination of the actions of a center load and a force pair (Figure 2). The boundary conditions of center loading are:

$$\left.\begin{array}{llll} \tau_{xy}=0 & y=0 & |x|<\infty & \\ \sigma_y=0 & y=0 & |x|<a & |x|>b \\ v=c\ (\text{常数}) & y=0 & a<|x|<b & \end{array}\right\} \qquad (1)$$

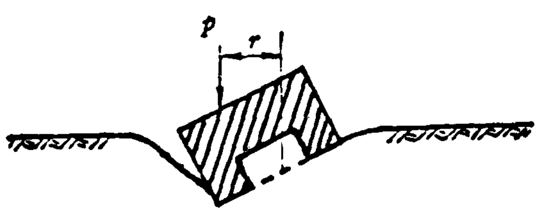

Figure 1

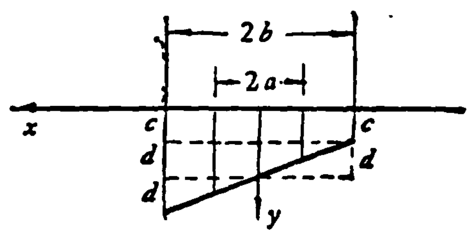

Figure 2

*This paper was received on November 7, 1978.

For the force pair, the boundary conditions are:

$$\left.\begin{array}{llll} \tau_{xy} = 0 & y = 0 & |x| < \infty & \\ \sigma_y = 0 & y = 0 & |x| < a & |x| > b \\ v = \frac{d}{b} x = \theta x & y = 0 & a < |x| < b & \end{array}\right\} \qquad (2)$$

where θ = d/b is the rotation angle of the footing.

The displacement and stress of the foundation can be expressed by the complex function ϕ(z):

$$\left.\begin{array}{l} 2\mu(u + iv) = \kappa\varphi(z) + \varphi(\bar{z}) + (\bar{z} - z)\overline{\varphi'(z)} \\ \sigma_x - \sigma_y + 2i\tau_{xy} = -2\{(z - \bar{z})\overline{\varphi''(z)} - \varphi'(\bar{z}) - \overline{\varphi'(z)}\} \\ \sigma_y - i\tau_{xy} = \varphi'(z) - \varphi'(\bar{z}) + (z - \bar{z})\overline{\varphi''(z)} \end{array}\right\} \qquad (3)$$

The solution of ϕ(z) which satisfies the boundary condition (1) is:

$$\varphi'(z) = -\frac{ipz}{2\pi X(z)} \qquad (4)$$

where $\kappa = \frac{\lambda + 3\mu}{\lambda + \mu}$, $X(z) = (z^2 - b^2)^{1/2}(z^2 - a^2)^{1/2}$, . The solution of ϕ(z) which satisfies the boundary conditions (2) is

$$\varphi'(z) = \frac{2\mu\theta i}{1 + \kappa}\left\{1 - \frac{z^2 - \frac{1}{2}(a^2 + b^2)}{X(z)}\right\} \qquad (5)$$

Under center loading conditions, the displacement of the footing can be obtained from (4) and (3):

$$u|_{y=0} = \frac{(\kappa - 1)p\beta}{4\pi}, \quad v|_{y=0} = -\frac{(1 + \kappa)}{4\pi\mu}\log A \qquad a < |x| < b \qquad (6)$$

where $A = (b^2 - a^2)^{1/2}$, $\beta = \operatorname{arctg}\frac{b\sin\omega}{(b^2\cos^2\omega - a^2)^{1/2}}$, $\omega = \arcsin\frac{(b^2 - x^2)^{1/2}}{b}$.

For footing under the action of a force pair M, the angle of rotation is:

$$\theta = \frac{(1 + \kappa)M}{2\pi\mu(b^2 - a^2)} \qquad (7)$$

The stress distribution on the bottom of the footing under center load conditions can be obtained from (4) and (3) as:

$$\left.\begin{aligned}\sigma_y|_{y=0} &= -\frac{px}{\pi(x^2-a^2)^{1/2}(b^2-x^2)^{1/2}} \qquad a<|x|<b\\ \tau_{xy}|_{y=0} &= 0\end{aligned}\right\} \tag{8}$$

Under the action of the force pair, from (5) and (3), we get:

$$\left.\begin{aligned}\sigma_y|_{y=0} &= \frac{2M}{\pi(b^2-a^2)}\,\frac{x^2-\frac{1}{2}(a^2+b^2)}{(x^2-a^2)^{1/2}(b^2-x^2)^{1/2}} \qquad a<|x|<b\\ \tau_{xy}|_{y=0} &= 0\end{aligned}\right\} \tag{9}$$

As for the stress distribution of the foundation under center loading, we obtain the following by substituting (4) into (3):

$$\left.\begin{aligned}\sigma_x &= \frac{p}{\pi}(\rho_0^1\rho_0^2\rho_1^1\rho_1^2)^{-1/2}\Big[(-A(x,y)+1)y\cos\frac{\varphi_0^1+\varphi_0^2+\varphi_1^1+\varphi_1^2}{2}\\ &\quad+(yB(x,y)-x)\sin\frac{\varphi_0^1+\varphi_0^2+\varphi_1^1+\varphi_1^2}{2}\Big]\\ \sigma_y &= \frac{p}{\pi}(\rho_0^1\rho_0^2\rho_1^1\rho_1^2)^{-1/2}\Big[(A(x,y)+1)y\cos\frac{\varphi_0^1+\varphi_0^2+\varphi_1^1+\varphi_1^2}{2}\\ &\quad-(yB(x,y)+x)\sin\frac{\varphi_0^1+\varphi_0^2+\varphi_1^1+\varphi_1^2}{2}\Big]\\ \tau_{xy} &= -\frac{py}{\pi}(\rho_0^1\rho_0^2\rho_1^1\rho_1^2)^{-1/2}\Big[A(x,y)\sin\frac{\varphi_0^1+\varphi_0^2+\varphi_1^1+\varphi_1^2}{2}\\ &\quad+B(x,y)\cos\frac{\varphi_0^1+\varphi_0^2+\varphi_1^1+\varphi_1^2}{2}\Big]\end{aligned}\right\} \tag{10}$$

where

$$\left.\begin{aligned}\rho_0^1 &= [(x-a)^2+y^2]^{1/2} \qquad \rho_0^2 = [(x+a)^2+y^2]^{1/2}\\ \varphi_0^1 &= \operatorname{arc\,tg}\frac{y}{x-a} \qquad \varphi_0^2 = \operatorname{arc\,tg}\frac{y}{x+a}\end{aligned}\right\} \tag{11}$$

$$\left.\begin{aligned}\rho_1^1 &= [(x-b)^2+y^2]^{1/2} \qquad \rho_1^2 = [(x+b)^2+y^2]^{1/2}\\ \varphi_1^1 &= \operatorname{arc\,tg}\frac{y}{x-b} \qquad \varphi_1^2 = \operatorname{arc\,tg}\frac{y}{x+b}\end{aligned}\right\} \tag{12}$$

$$\left.\begin{aligned}A(x,y) &= [(x^2-y^2-b^2)(x^2-y^2-a^2)-4x^2y^2][(x^2-y^2)^2-4x^2y^2-a^2b^2]\\ &\quad+8x^2y^2(x^2-y^2)[2(x^2-y^2)-(a^2+b^2)]/[(x^2+y^2)^2\\ &\quad-2(x^2-y^2)b^2+b^4][(x^2+y^2)^2-2(x^2-y^2)a^2+a^4]\\ B(x,y) &= 2xy[(a^2+b^2)(x^2+y^2)^2-4a^2b^2(x^2-y^2)+a^2b^2(a^2+b^2)]/\\ &\quad[(x^2+y^2)^2-2(x^2-y^2)b^2+b^4][(x^2+y^2)^2-2(x^2-y^2)a^2+a^4]\end{aligned}\right\} \tag{13}$$

Under the action of the force pair, we get the following by substituting (5) into (3):

$$
\left.\begin{aligned}
\sigma_x &= \frac{M}{\pi(b^2-a^2)}(\rho_0^1\rho_0^2\rho_1^1\rho_1^2)^{-1/2}\Big\{[(b^2-a^2)^2C(x,y)-4x]y\cos\frac{\varphi_0^1+\varphi_0^2+\varphi_1^1+\varphi_1^2}{2} \\
&\quad+\left[2\left(x^2-y^2-\frac{1}{2}(a^2+b^2)\right)-(b^2-a^2)^2yD(x,y)\right]\sin\frac{\varphi_0^1+\varphi_0^2+\varphi_1^1+\varphi_1^2}{2}\Big\} \\
\sigma_y &= -\frac{M}{\pi(b^2-a^2)}(\rho_0^1\rho_0^2\rho_1^1\rho_1^2)^{-1/2}\Big\{[(b^2-a^2)^2C(x,y)+4x]y\cos\frac{\varphi_0^1+\varphi_0^2+\varphi_1^1+\varphi_1^2}{2} \\
&\quad-\left[2\left(x^2-y^2-\frac{1}{2}(a^2+b^2)\right)+(b^2-a^2)^2yD(x,y)\right]\sin\frac{\varphi_0^1+\varphi_0^2+\varphi_1^1+\varphi_1^2}{2}\Big\} \\
\tau_{xy} &= \frac{M(b^2-a^2)}{\pi}(\rho_0^1\rho_0^2\rho_1^1\rho_1^2)^{-1/2}y\Big[C(x,y)\sin\frac{\varphi_0^1+\varphi_0^2+\varphi_1^1+\varphi_1^2}{2} \\
&\quad+D(x,y)\cos\frac{\varphi_0^1+\varphi_0^2+\varphi_1^1+\varphi_1^2}{2}\Big]
\end{aligned}\right\}\quad(14)
$$

where

$$
\left.\begin{aligned}
C(x,y) &= \frac{x[(x^2-y^2)^2-4y^4-(x^2+y^2)(a^2+b^2)+a^2b^2]}{[(x^2-y^2-b^2)^2+4x^2y^2][(x^2-y^2-a^2)^2+4x^2y^2]} \\
D(x,y) &= \frac{y[4x^4-(x^2-y^2)^2-(x^2+y^2)(a^2+b^2)-a^2b^2]}{[(x^2-y^2-b^2)^2+4x^2y^2][(x^2-y^2-a^2)^2+4x^2y^2]}
\end{aligned}\right\}\quad(15)
$$

Figures 3 and 4 show the stress distribution σ_y on a few horizontal surfaces under center loading and force pair conditions respectively. Each figure only shows half of the entire picture. The other half of Figure 3 is symmetric to what is shown. For Figure 4, the half nut shown is asymmetric to what is presented.

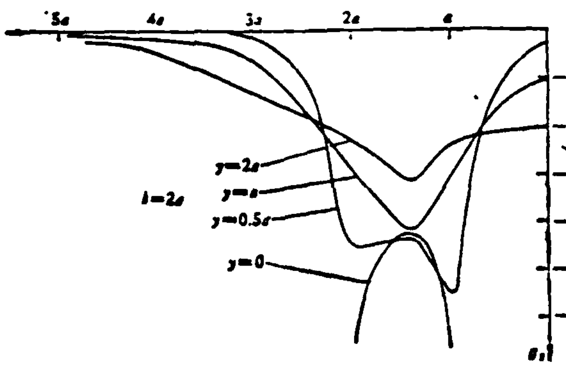

Figure 3

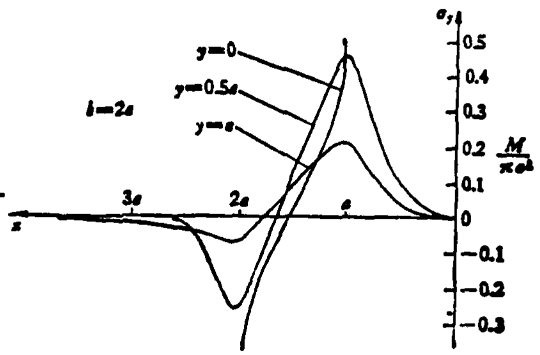

Figure 4

From (6), (7) and (8), we can see that when a = 0, the following holds for long solid rigid frame footings:

$$u|_{y=0} = \frac{(\kappa - 1)p\omega}{4\pi\mu}, \qquad v|_{y=0} = -\frac{(1+\kappa)p}{4\pi\mu}\log b, \qquad |x| < b,$$
$$\theta = \frac{(1+\kappa)M}{2\pi\mu b^2}, \qquad \sigma_y|_{y=0} = -\frac{p}{\pi(b^2 - x^2)^{1/2}}, \qquad |x| < b,$$

Our results are consistent with those found by Galin [1], Muskhelishvili [2] and Sneddon [3].

From (9) and Figure 4, we see that $\sigma_y|_{y=0}$ changes signs between -b and -a and a and b. This implies that tensile stress will appear at some location on the bottom of the footing. When the footing does not adhere to the foundation or when the adhesion is less than the tensile force, the footing will be detached from the foundation. Therefore, in order to avoid such a detachment effect, the load and its corresponding force pair must satisfy certain relations.

From (8) and (9), we get the stress distribution on the bottom of the footing under off-center load:

$$\sigma_y|_{y=0} = -\frac{px}{\pi(x^2 - a^2)^{1/2}(b^2 - x^2)^{1/2}} + \frac{2M}{\pi(b^2 - a^2)}\,\frac{x^2 - \frac{1}{2}(a^2 + b^2)}{(x^2 - a^2)^{1/2}(b^2 - x^2)^{1/2}}, \quad a < |x| < b$$

It is well known that in order not to allow detachment of the footing from the foundation, it is necessary to make the normal stress on the bottom of the footing be pressure stress. Therefore,

$$\frac{2M}{(b^2 - a^2)}\,\frac{x^2 - \frac{1}{2}(a^2 + b^2)}{(x^2 - a^2)^{1/2}(b^2 - x^2)^{1/2}} \leqslant \frac{px}{(x^2 - a^2)^{1/2}(b^2 - x^2)^{1/2}}, \quad a < |x| < b$$

and

$$M \leqslant p(a + b)/2 \qquad (16)$$

If the action point of load is a distance r off-center (see Figure 1), then M = rp. From this the equation that r must satisfy so that the footing and the foundation will not separate is:

$$r \leqslant (a + b)/2 \qquad (17)$$

For long solid frame footing, a = 0, and the above becomes:

$$M \leqslant pb/2, \qquad r \leqslant b/2$$

This is consistent with result obtained by Muskhelishvili

REFERENCES

[1] Ganin, P. A., (translated by Wang Chun Xen) "Contact Problems in Elastic Theory", Science Publication, 1958.

[2] Muskhelishvili, N. I., Some Basic Problems of the Mathematical Theory of Elasticity P. Noordhoff Ltd., (1963).

[3] Sneddon, I. N., Fourier Transforms, New York, McGraw-Hill, (1951).